

AWARD NUMBER: W81XWH-16-2-0002

TITLE: Central Mechanisms and Treatment of Blast-Induced Auditory and Vestibular Injuries

PRINCIPAL INVESTIGATOR: Dr. Joseph B. Long

RECIPIENT: The Geneva Foundation, Tacoma, WA

REPORT DATE: October 2021

TYPE OF REPORT: Final Report

PREPARED FOR: U.S. Army Medical Research and Materiel Command
Fort Detrick, Maryland 21702-5012

DISTRIBUTION STATEMENT: Approved for Public Release; Distribution Unlimited

The views, opinions and/or findings contained in this report are those of the author(s) and should not be construed as an official Department of the Army position, policy or decision unless so designated by other documentation.

REPORT DOCUMENTATION PAGE*Form Approved*
OMB No. 0704-0188

Public reporting burden for this collection of information is estimated to average 1 hour per response, including the time for reviewing instructions, searching existing data sources, gathering and maintaining the data needed, and completing and reviewing this collection of information. Send comments regarding this burden estimate or any other aspect of this collection of information, including suggestions for reducing this burden to Department of Defense, Washington Headquarters Services, Directorate for Information Operations and Reports (0704-0188), 1215 Jefferson Davis Highway, Suite 1204, Arlington, VA 22202-4302. Respondents should be aware that notwithstanding any other provision of law, no person shall be subject to any penalty for failing to comply with a collection of information if it does not display a currently valid OMB control number. **PLEASE DO NOT RETURN YOUR FORM TO THE ABOVE ADDRESS.**

1. REPORT DATE October 2021		2. REPORT TYPE Final		3. DATES COVERED 30Dec2015 - 29Jun2021	
4. TITLE AND SUBTITLE Central Mechanisms And Treatment Of Blast-Induced Auditory and Vestibular Injuries				5a. CONTRACT NUMBER	
				5b. GRANT NUMBER W81XWH-16-2-0002	
				5c. PROGRAM ELEMENT NUMBER	
6. AUTHOR(S) Dr. Joseph B. Long E-Mail: joseph.b.long.civ@mail.mil				5d. PROJECT NUMBER 10442	
				5e. TASK NUMBER	
				5f. WORK UNIT NUMBER	
7. PERFORMING ORGANIZATION NAME(S) AND ADDRESS(ES) The Geneva Foundation 917 Pacific Ave, Suite 600 Tacoma, WA 98402				8. PERFORMING ORGANIZATION REPORT NUMBER	
9. SPONSORING / MONITORING AGENCY NAME(S) AND ADDRESS(ES) U.S. Army Medical Research and Materiel Command Fort Detrick, Maryland 21702-5012				10. SPONSOR/MONITOR'S ACRONYM(S)	
				11. SPONSOR/MONITOR'S REPORT NUMBER(S)	
12. DISTRIBUTION / AVAILABILITY STATEMENT Approved for Public Release; Distribution Unlimited					
13. SUPPLEMENTARY NOTES					
14. ABSTRACT The study is to utilize our well-defined shock tube simulation of mild blast-induced traumatic brain injury (bTBI) in rodents to characterize interrelated biomechanical and pathophysiological mechanisms of blast-induced central auditory processing disorders and central vestibular injuries and to develop an early therapeutic intervention for hearing loss and balance disorder mitigation. The major objectives of the proposed studies and relevant research sub-gaps are: 1) Verify the time course of hearing loss and balance disorders induced by blast exposure and define plasma and CSF TDP-43 as a biomarker related to blast-induced central auditory/vestibular deficits; 2) Characterize blast induced biochemical, functional and morphological alterations in central auditory/vestibular systems and establish that blast-induced altered expression of TDP-43 and its BDPs in these structures play a key pathophysiological mechanism leading to secondary injuries.					
15. SUBJECT TERMS Traumatic brain injury					
16. SECURITY CLASSIFICATION OF:			17. LIMITATION OF ABSTRACT	18. NUMBER OF PAGES	19a. NAME OF RESPONSIBLE PERSON
a. REPORT Unclassified	b. ABSTRACT Unclassified	c. THIS PAGE Unclassified	Unclassified	25	USAMRMC
					19b. TELEPHONE NUMBER (include area code)

Standard Form 298 (Rev. 8-98)
Prescribed by ANSI Std. Z39.18

TABLE OF CONTENTS

	<u>Page No.</u>
1. Introduction	4
2. Keywords	4
3. Accomplishments	4
4. Impact	23
5. Changes/Problems	23
6. Products	23
7. Participants & Other Collaborating Organizations	24
8. Special Reporting Requirements	25
9. Appendices	25

1. INTRODUCTION:

With widespread use of improvised explosive devices in recent military conflicts, blast-induced traumatic brain injury (bTBI) and neurosensory dysfunction have emerged as key military medical issues. Auditory and vestibular disorders are particularly prevalent, and the debilitating consequences of these injuries likely progress with age. A comprehensive understanding of the structural and molecular components of the injury is essential for the development of the most appropriate therapies for auditory and vestibular deficits resulting from blast exposure. Existing data indicate that both the inner ear and the structures in the brain responsible for auditory and vestibular function are at high risk of injury following blast exposure. The ongoing study utilizes an Advanced Blast Simulator (ABS) to recreate these injuries in rodents in the laboratory. Through comprehensive assessments of the resultant auditory and vestibular deficits using a battery of functional tests in conjunction with characterizations of the underlying biochemical and anatomical changes in these structures, the interrelated biomechanical and pathophysiological mechanisms responsible for blast-induced central auditory processing disorders and central vestibular injuries are being elucidated and will provide therapeutic targets for hearing loss and balance disorder mitigation.

2. KEYWORDS:

mouse, blast, injury, auditory cortex (AC), medial geniculate nucleus (MGN), cerebellum, brainstem, electrophysiology, pathology, dendritic spines, synaptic plasticity, RNAseq, proteomics

3. ACCOMPLISHMENTS:

○ What were the major goals of the project?

The major objective for the project were: (1) to verify the time course of central auditory processing disorders and vestibular injuries induced by blast exposure and definition of time-dependent changes in TDP-43 in plasma as a biomarker related to blast-induced central auditory/vestibular deficits; (2) to characterize blast injury to primary auditory cortex and brainstem/cerebellum associated with central auditory processing disorders and central vestibular injuries; (3) to define blast-induced altered expression of TDP-43 as a key pathophysiological mediator leading to the secondary central auditory and vestibular processing injuries.

○ What was accomplished under these goals?

1) Major activities

- In the study period, we have defined a suitable mouse model of blast-induced mild traumatic brain injury (bTBI) that can demonstrate some pathological changes consistently among individual animals.
- We have successfully assessed the impact of shockwave on auditory function including sound signal generation and transduction by testing the distortion products of otoacoustic emissions (DPOAE) and auditory brainstem responses (ABR), as well as employing whole-cell patch-clamp recording at the auditory cortex.
- We have successfully conducted a microinjection technique for targeting the medial geniculate nuclei (MGN) in mouse.

- We have determined blast-induced cortical neuronal morphological changes by analyzing the dendritic spines using Thy1-YFP mice, and also evaluated the axonal degeneration by silver staining.
- We also performed single cell RNA sequencing (scRNA-seq) analyses to examine the regulation of TDP-43 target genes in the individual neurons.
- We also determined blast-induced molecular by analyzing the proteomics profiles.
- We also validated blast-induced differentially expressed proteins in the cortex by Western blot or ELISA
- We assessed the effects of shockwave on cytokines using magnetic bead kits

2) Specific Objectives

- I. Establish a mouse bTBI model
- II. Evaluate auditory deficits following blast exposures
 1. ABR and DPOAE
 2. Functional connectivity in central auditory/vestibular systems
 - Assessment of functional connectivities between MGN and AC
 - Assessment of functional connectivity between FL and LVe
- III. Determine blast-induced neuronal morphological changes
 1. Effects of blast on post synaptic structures
 2. Effects of blast exposure on presynaptic structures
 3. Blast-induced pathological changes in brainstem and cerebellum
- IV. Define the role of TDP-43 in neurons
 1. Effects of shockwave on TDP-43 changes in the brain
 2. Verify overexpression of TDP-43 altered neuronal development in cultured neurons
 3. Examine the regulation of TDP-43 target genes in the single neurons of thalamus
- V. Determine blast-induced protein changes in the cortex and cerebellum
 1. Proteomic characterization of the proteomes in the cortex
 2. Proteomic characterization of the proteomes in the cerebellum
 3. Validation of blast-induced DEPs in the cortex by Western blot or ELISA

3) Significant Results (major findings, development, or conclusions)

I. Mouse bTBI model

Although we established a mouse bTBI model using an older constant diameter shock tube, the effects of blast exposure generated in an advanced blast simulator (ABS, fig. 1) which eliminates numerous artefacts confounding constant diameter tube exposures, had not been investigated prior to the initiation of this study. The severity of blast injury can be affected by a type of shock tube, pressure, unnumber of blasts, blast interval, anaesthesia and animal position. Therefore, a pilot study was necessary for selection of an appropriate animal model in the proposed research.

Based on our previous experiences, mice exposed to three tightly coupled blast exposures in an old shock tube showed greater prolonged unconsciousness and more severe brain injury than was produced by a single exposure (Wang et.al., 2011), we selected the following experimental groups: single blast (BOP), two repeated blasts (BOP2), three repeated blasts (BOP3) and sham controls (Sham), as well as noise controls (NC). Mice (male, 23 - 28 g, age of 9 – 11 weeks) were secured in the ABS in a prone position facing the oncoming shockwave immediately after administration of 4% isoflurane gas anesthesia in an induction chamber for 8 min (O2 flow rate 1.5L/min). For BOP2, mice received additional isoflurane anesthesia for 2 min immediately following the first exposure and were then exposed to the second blast shockwave. For BOP3, mice immediately received additional isoflurane anesthesia for 2 min separating the second and third blast exposures. Sham control animals were included in all individual experiments and were treated in the same fashion without exposure to blast shockwaves. The blast overpressure (peak static pressure of 19 psi and 4 msec positive phase duration) was generated by Valmex membrane rupture in the ABS which consists of a 0.5 ft long compression chamber that is separated from a 21 ft long transition/expansion test section.

The comparison of righting reflex time (RRT) among experimental groups of Sham = 30, Sham2 = 8, Sham3 = 8, NC = 9, BOP = 30, BOP2 = 10 and BOP3 = 30 are displayed in figure 2. Data showed that RRT increased significantly in blast treated groups, while there were no difference among sham controls as well as between sham and noise exposed mice. Compared to BOP, BOP2 and BOP3 caused a significant elevation of RRT ($p < 0.0001$), respectively. There was no significant change between BOP2 and BOP3. The mortality was 7.5% for BOP and 11.8% for BOP3.



Fig. 1. The Advanced Blast Simulator (ABS)

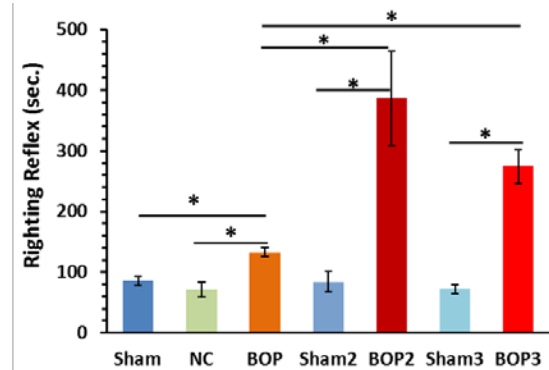


Fig. 2. Righting reflex time after exposure to ABS

II. Auditory deficits following blast exposures

Theoretically, auditory functional deficits can result any impairment in ear and neural connections from brainstem to thalamus and cortex. The most recognized reliable and sensitive measurement for auditory function assessment are auditory brainstem responses (ABRs) and distortion products of otoacoustic emissions (DPOAE). For assessment of connectivity between medial geniculate nuclei (MGN) and auditory cortex (AC), we used

a combination technologies of whole-cell patch-clamp electrophysiological recording with optogenetics.

II-1. ABR and DPOAE

CBA mice are commonly used in ear studies and C57BL mice have been reported to possibly have an age-related ABR change. However C57BL mice have been recognized as a good strain for genetic and neurobehavioral research. Therefore both strains of mice had been investigated.

ABR thresholds across the frequency ranges from 8 kHz through 40 kHz were assessed before (as the baseline) and after blast exposure in CBA mice. Baseline mean ABR thresholds were between 20-30 dB SPL for all frequencies tested. One day after blast exposure, the right ear (70%) had no ABR response at the maximum stimulus level of 90 dB SPL (Fig. 3a), while left ear exhibited average threshold shifts of ~75-85 dB SPL at 8 kHz and 16 kHz (Fig. 3b). However, there was no statistical difference between right and left ear measurements. Reduction of blast-elevated ABR thresholds were apparent at 7 days post injury, and significant differences were found at 14, 21 and 28 days post blast (Fig. 3c, 3d).

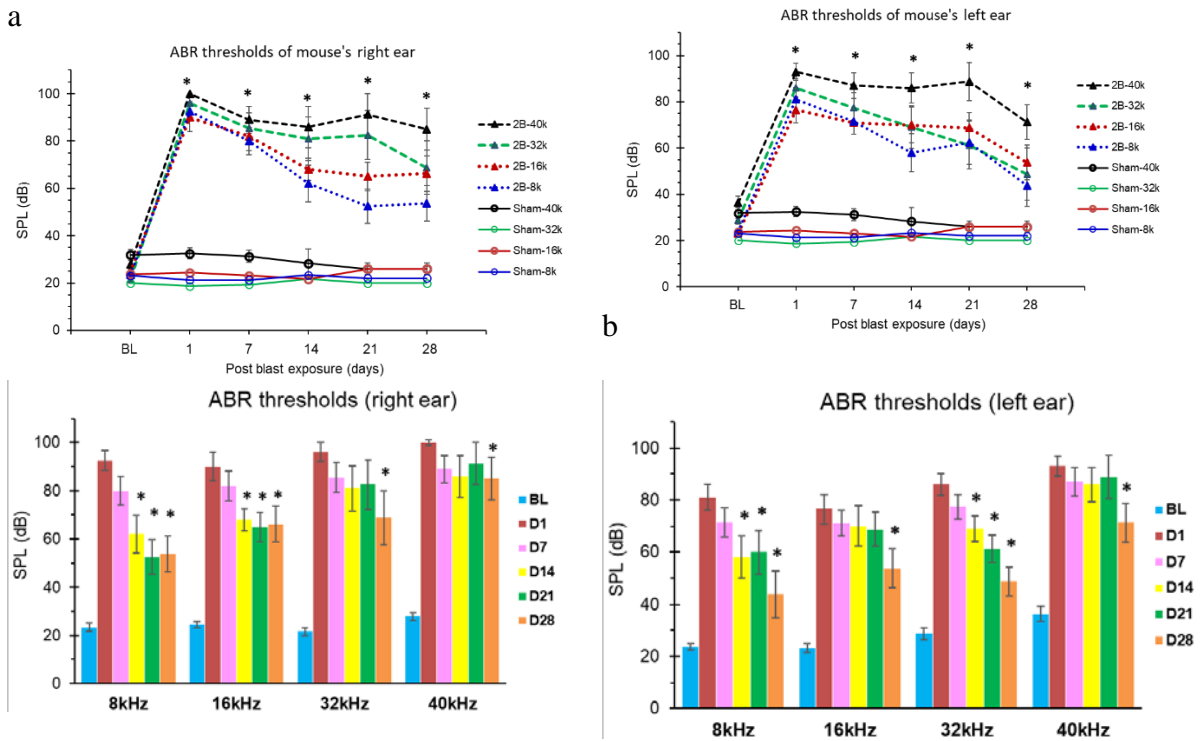


Fig. 3. Elevated ABR thresholds in all frequency ranges following two repeated blast exposures

Similar to the CBA mice, C57BL mice presented significant ABR threshold shifts (Fig. 4) induced by blast exposure. A complete hearing loss (threshold > 90 dB) was observed at 1 day after repeated blast exposures, and these deficits persisted over 3 months. Compared to the sham controls, blast-induced elevation of ABR threshold was evident throughout the whole spectra of sound frequencies. At 14 days after injury, the ABR threshold to lower frequency (8 kHz) stimuli indicated a partial recovery of hearing.

In contrast, the ABR threshold to higher frequency (40 kHz) stimuli did not recover through 90 days post-injury.

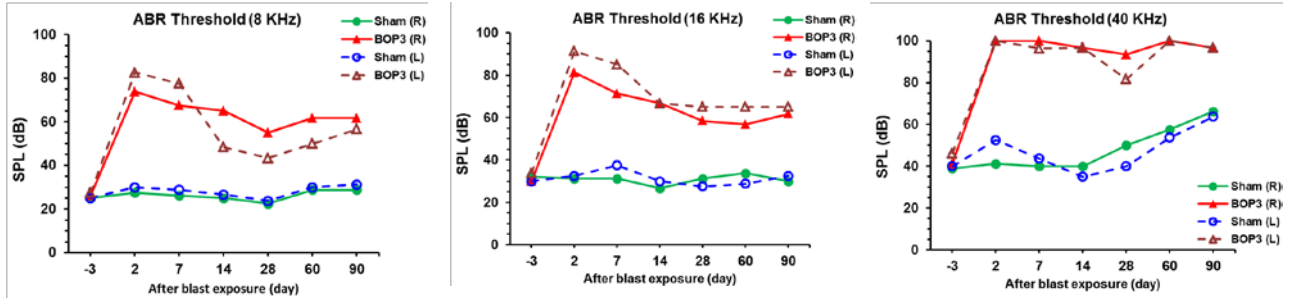


Fig. 4. Effects of three blast exposures on ABR threshold in C57BL/6 mice.

DPOAEs reflect the condition of hair cells in the inner ear. Absence of DPOAEs were determined at a higher frequency range of 22 – 40 kHz from 1 day up to 28 days post blast (Fig. 5). At 1 day post blast, very small DPOAEs at 8 kHz may be recorded from 15% of mice that received single blast exposure (BOP). DPOAEs often recovered over time. For BOP2 mice, DPOAEs at 8 kHz can be detected at 14 days post blast. In contrast, no DPOAEs were detected in BOP3 mice prior to 180 days (data are not shown). These results indicate that the impact of blast exposure on high frequency (40 kHz) hearing was severe and persistent.

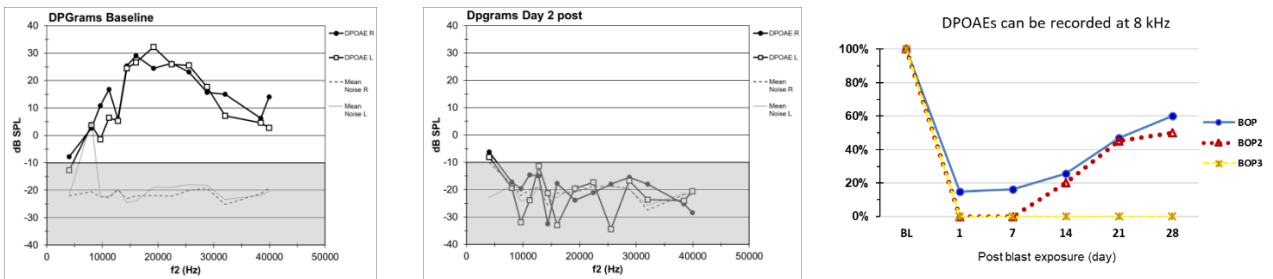


Fig. 5. DPOAEs were absent following blast exposure in CBA mice.

II-2. Functional connectivity in central auditory/vestibular systems

Auditory functional deficits can result from any impairment in neural connections from brainstem to thalamus and cortex. Neurons and glia are functionally organized into circuits and higher-order structures via synaptic connectivity and activity-dependent refinement. It is known that medial geniculate nuclei - auditory cortex (MGN - AC) projections plays a critical role in sound processing, while flocculus - lateral vestibular nuclei (FL - LVe) projections plays a critical role in body balance regulation. To determine whether blast impaired neural connectivities in the brain, the optogenetics assay was performed in combination with whole-cell patch-clamp electrophysiological recording.

Assessment of functional connectivity between MGN and AC: We met two technical challenges associated with virus injection and cell patch recording when carrying out this study. 1) a precise region for the viral injection, since there is no available brain map for an immature (age of 5 weeks) mouse, 2) the structures in different brain regions influence the whole cell patching.

After analyzing the pilot data, we confirmed that the time period of 3-4 weeks following viral injection is necessary for expression of yellow fluorescence protein. Blast treatment was designed to apply to the mice at age of 9 – 10 weeks. We successfully observed green fluorescence within the AC region after injection of adeno-associated virus encoded with CAG-ChR2-YFP genes into the MGN (Fig. 6a). Briefly, after 4 weeks recovery from the surgery, mice were then anesthetized and received either closely coupled repeated blast exposures (peak static pressure of 16 psi and 4 msec positive phase duration) in the advanced blast simulator or sham handling. Brain slices (300 μm) were prepared and used for whole-cell patch-clamp recordings at 1, 3 and 7 days and 1 month post-injury. Recording was done under visual guidance using an Olympus BX51 microscope equipped with both transmitted light illumination and epifluorescence illumination. The blue light-induced EPSCs were recorded from layer IV neurons in the AU with a holding potential at -70 mV (Fig. 6b).

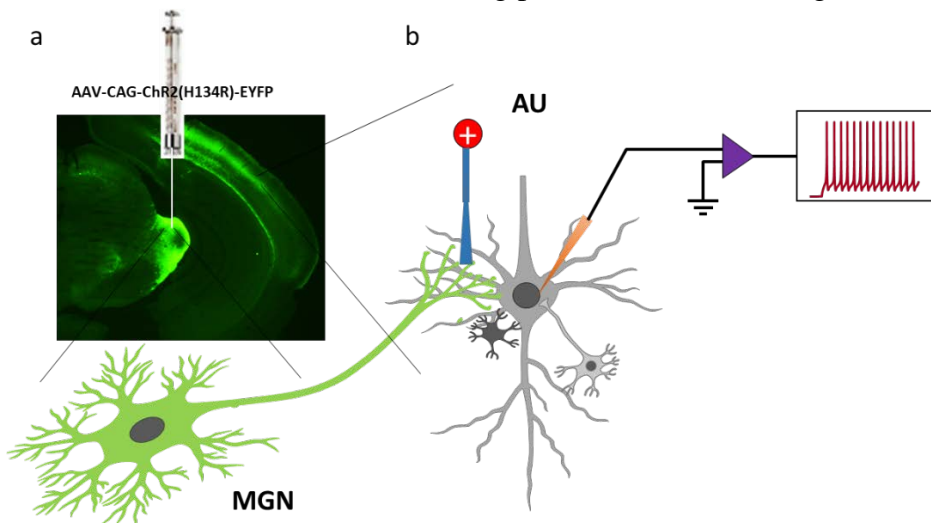


Fig. 6. Schematic diagram of the viral injection (a) and whole-cell patch-clamp recording with optogenetics (b)

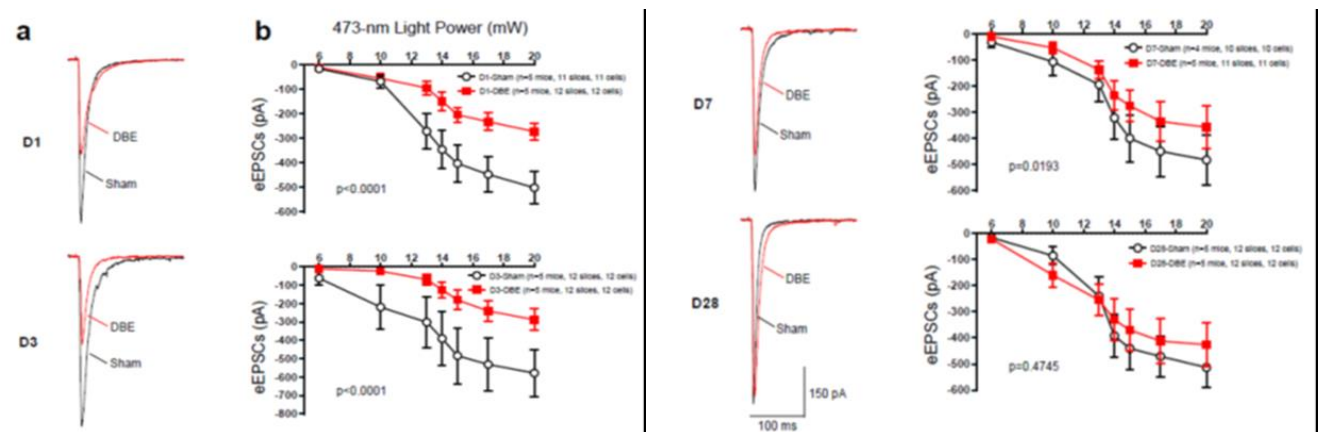


Fig.7. Impaired MGN-AU synaptic transmission in the blast mouse model

The results showed (Fig. 7) that input–output relationships between stimulation intensity and EPSCs at the MGN-AU projections in the AU were significantly reduced at

1, 3 and 7 days after blast exposures (two-way ANOVA, $p < 0.0001$, $p < 0.0001$, and $p = 0.0193$, respectively). There were no significant changes at 1 month (28 – 30 days) after the repeated blast exposures, indicating an apparent recovery (i.e. plasticity) from abnormal circuits among neurons and glia. These results reveal that closely coupled shockwaves impaired sound signal processing centers, which potentially contribute to hearing deficits in acute and sub-acute injury phases. In addition to highlighting perturbations potentially underlying blast-induced auditory dysfunction, these findings also provide potential insights into optimal therapeutic window after blast exposures in patients.

Assessment of functional connectivity between FL and LVe: The impaired functional connectivity between FL and LVe may be a potential mechanism associated with balance disorders after blast exposure. However, we encountered three technical challenges while carrying out research to explore this possibility. They were 1) expression both of channelrhodopsin-2 (ChR2) and fluorescent protein (YFP) in the Purkinje cell (PC), 2) precise expression of ChR2-YFP in the FL that projects to LVe, and 3) whole cell recording on the neurons in LVe.

The first challenge stemmed from the requirement to generate an adeno-associated virus encoded ChR2-YFP gene. Unlike the study of functional connectivity between MGN and AC, there is no commercial agent available for study in the cerebellum. AAV-CAG-ChR2-YFP does not selectively express in the Purkinje cells. The L7/pcp-2 is a known specific promoter for the PC. Technically, we can use L7 replace CAG to get the AAV-L7-ChR2-YFP, but the original size of L7 is 3100 bp which is too big to be constructed into the final product. Therefore, we had to truncate Δ L7 to 1000 bp. To test whether the Δ L7 expresses in cells, we successfully generated AAV- Δ L7-YFP and verified its expression in the cultured primary neurons. Additionally, ChR2 is a patented item that can be used by the authorized institute. After signed a material transfer agreement, the the Δ L7 plasmid was delivered to UPENN core facility to generate AAV- Δ L7-ChR2-YFP.

Injection of AAV- Δ L7-ChR2-YFP into the FL region was very challenging. Part of the FL is located inside of the temporal bone and near the 4th ventricle. Precise atlases for a young mouse are rare and as a result, the success rate was low. After a preliminary study based upon a measurement of FL by dye injection, the location of -1.4 mm from lambda, 2.8 mm lateral and 2.8

vertical was used for 4 – 5 weeks old mice. Mice were anesthetized with isoflurane and received a 1 μ l AAV- Δ L7-ChR2-YFP into the FL. After 4 weeks fully recovery, mice received repetitive blast exposures or sham handling and were then euthanized at a variety of time points (1d, 3d, 7d and 28d) after bTBI. The FL-LVe slices (300 μ m) were cut into coronal sections and incubated in a Ringer solution. To record inhibitory

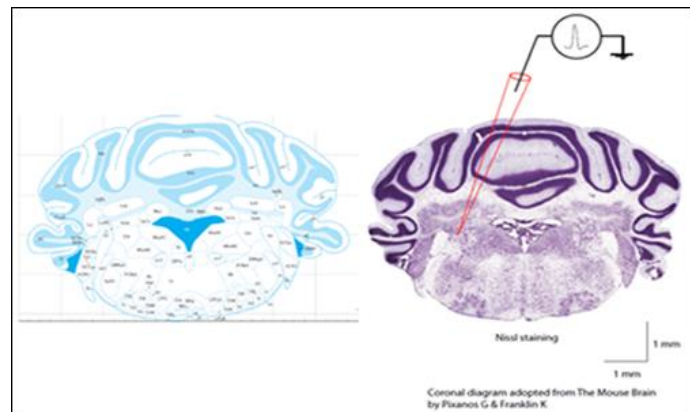


Fig. 8. Whole-cell patch clamp recording from lateral vestibular nucleus

postsynaptic currents (IPSCs), a different Cs⁺-based intracellular solution was used in the presence of 50 μM CNQX (Sigma) and 50 μM D-APV (Sigma) to block AMPA currents and NMDA currents, respectively. Whole-cell recordings were intended from cell bodies of LVe neurons with optogenetic stimulation (Fig.8). However, as illustrated in the figure above, only a few sparse neurons located in LVe were found within white matter of the brainstem although there the FL bundle with eYFP projecting to LVe was evident. Consequently, it was very difficult to establish a successful whole-cell patch recording configuration and we were ultimately forced to abandon this portion of the study due to technical limitations with this electrophysiological approach despite a considerable investment of time and resources. To investigate functional connectivity between FL and LVe after bTBI in future studies, it might be more fruitful to employ brain imaging methods such as fiber photometry or/and inscopix system with GCAP6 as alternative approaches.

III. Blast-induced neuronal morphological changes

III-1. Effects of blast on post synaptic structures

Precise sensory information processing requires complex interactions between neurons. The quantities and shapes of dendritic spines are correlated with the strength of synaptic transmissions that are associated with the function of particular neural networks. We focused on the auditory cortex which is one of the key units of sound processing.

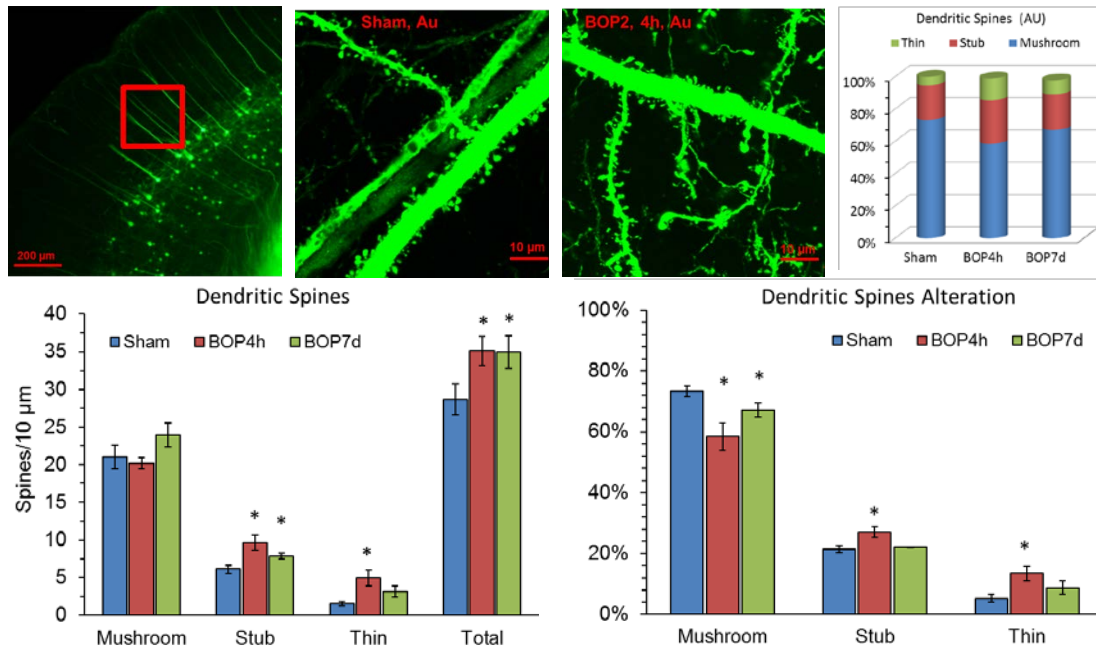


Fig. 9. Effect of blast exposure on dendritic spine in the auditory cortex

The Thy1-YFP transgenic mouse, provided by Jackson Laboratory, expresses yellow fluorescent protein at high levels in the cortical layer V pyramidal neurons. Compared to the sham controls, total numbers of dendritic spines in auditory cortex increased at 4 hr and 7d after blast exposure (Fig. 9). Those changes were predominantly in the immature types of stubby and thin spines, with no significant change observed in the number of

mushroom type. Consequently, the ratio of mushroom type spines decreased. The increase in the stub type of spine persisted to 7 days post-injury. The results indicated the synaptic transmissions in excitatory neurons were quite sensitive to blast insult.

III-2. Effects of blast exposure on presynaptic structures

To determine whether presynaptic boutons and branches are impacted by the shockwaves, the Thy1-RFP transgenic mice, provided by Jackson Laboratory, received injection of 1 ul AAV-CAG-GFP in the MGN (Fig. 10). After 4 weeks recovery, mice were selected randomly into a blast treatment group or a sham group. At designated time points, mice were euthanized and fixed in 4%PFA solution. Mouse brains were then dissected and cut coronally. The brain sections (80 μm) were mounted on glass slides. Images of the auditory cortex (AU) in each section were prepared using an Olympus confocal microscope and contained 30

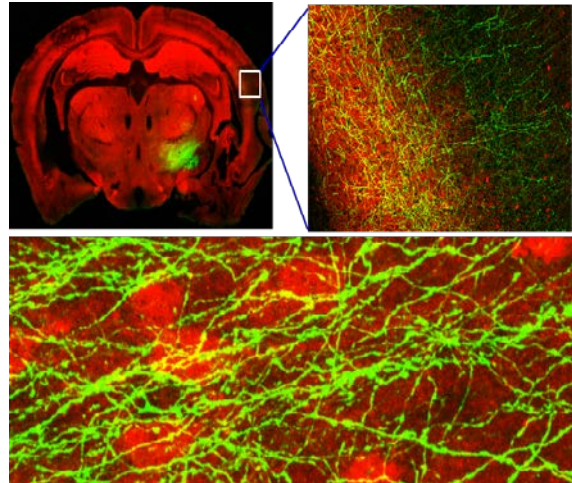


Fig. 10. Injection of aav-GFP to the MGN of Thy1-RFP mouse

– 50 areas with 40 z-stack pictures for each area. Imaris software was used for analyzing axonal plasticity. Data showed (Fig. 11) that axons in the AC region increased at 3 days post exposure in branch level (23%) and branch depth (100%), but decreased with regard to the number of synaptic knobs (24%) and terminal bouton volume (35%) comparing to the sham control. The result from colocalization analysis (merged colors) between synaptic bouton (green) and post-synaptic neurons (red) indicated the colocalized area was less than 18% in blasted mice.

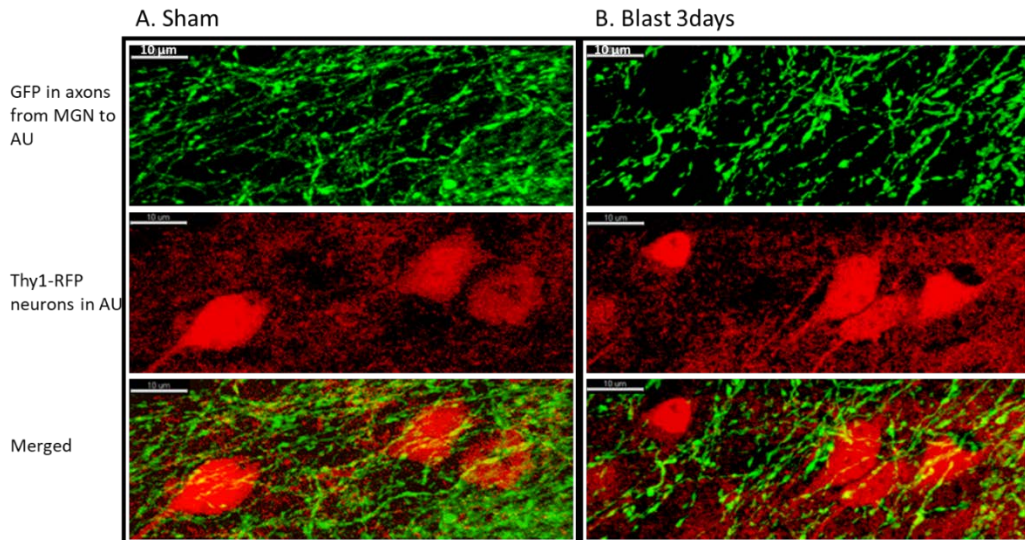


Fig. 11. Representative cryostat sections (80 μm thick) of sham and at 3 days post-blast.

Consistent with the long-range functional connectivity changes between MGN and AC, the morphologies of postsynaptic and presynaptic structures were also altered at 1, 3 and 7 days bTBI.

III-3. Blast-induced pathological changes in cerebellum and brainstem

To evaluate blast damage to CNS, we used silver staining and immunostaining, traditional technical means of microscopic analysis. Antibodies to GFAP (#3670, cell signaling) and Iba1 (#01919741, Wako chemicals) were used for immunohistochemistry analysis. As illustrated in the Fig. 12, the effect of shockwaves on axons and glial cells were evident in cerebellum (a, b, e and f) and brainstem (c, d, g and h) at 14 days post exposures. Compared to sham control (a – d), blast exposure causes axonal degeneration (e) along with increased Iba1 (f, g) and GFAP (h) immunoreactivity, scale bar 100 μ m. Data showed prominent axonal degeneration in the white matter of cerebellum (which was detected by silver staining) and the proliferation of microglia and astrocytes in the cerebellum and brainstem regions (which were visualized by anti-Iba1 and anti-GFAP immunostaining, respectively).

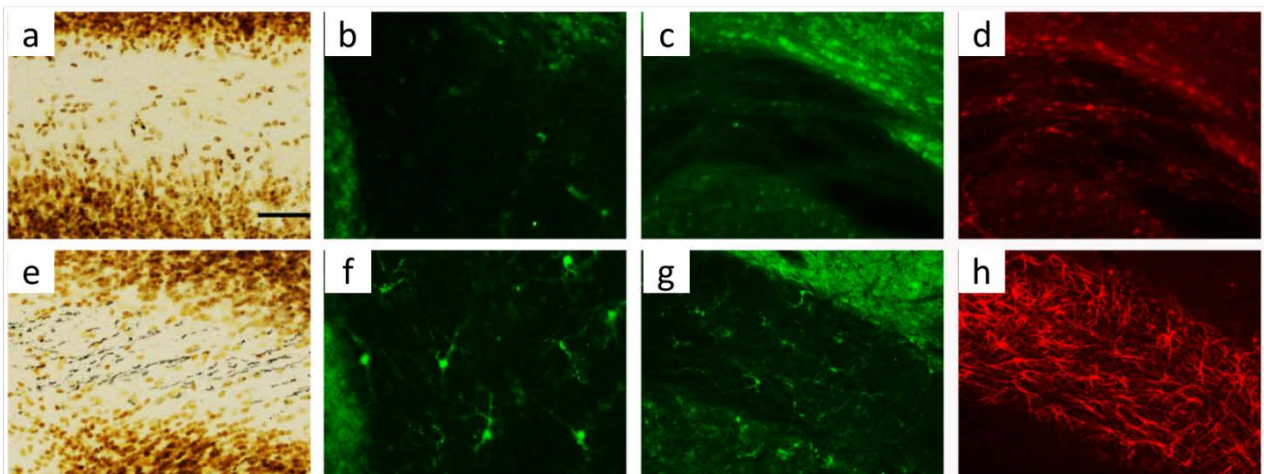


Fig. 12. Pathological changes in cerebellum and brainstem after blast exposure

IV. Define the role of TDP-43 in neurons

IV-1. Effects of shockwave on TDP-43 changes in the brain

TAR DNA-binding protein TDP-43 are evident in the brains of patients that present across a spectrum of neurodegenerative diseases. To determine whether blast causes TDP-43 change, we assessed the protein levels in different brain regions and plasma, using ELISA kits (MyBiosources.com). Compared to the sham group, TDP43 increased significantly in the cortex and brainstem of mice at 28 days after blast exposure ($p < 0.05$, $n = 10$). TDP-43 levels increased slightly, but no statistically significant differences were seen in the cerebellum and plasma (Fig.13a). TDP-43 level was not found to be significantly changed in the acute phase (1 day) after blast exposure. We selected a few antibodies that target TDP-43 at full length (eg. ab42474, abcam), N-terminal (sc376133, Santa Cruz and ab109535, abcam) or C-terminal (PA520408 and PA116996, Thermofisher) to verify the

alterations by analyzing immunoblotting data and/or immunohistochemistry (Fig.13b). The results were not very convincing due to the large variation among sham subjects.

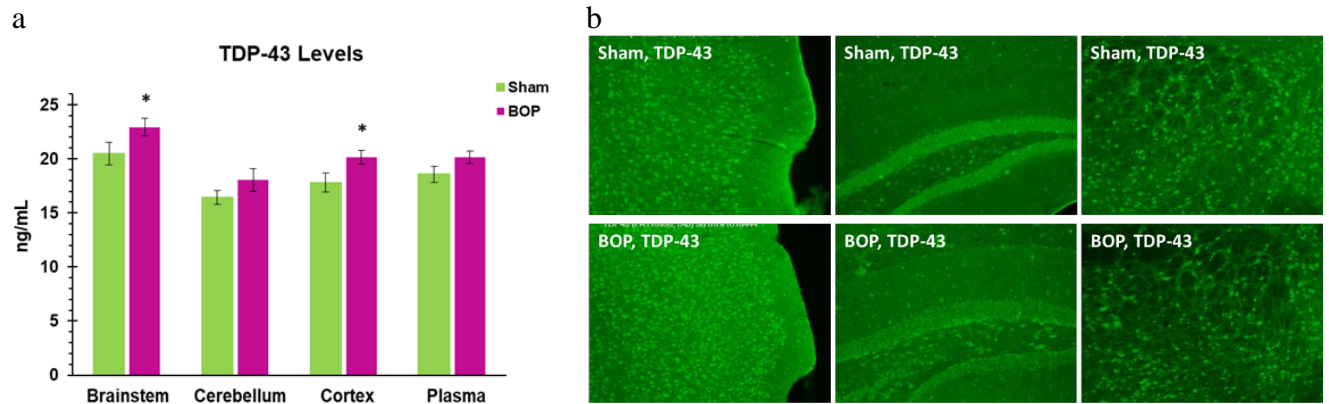


Fig. 13. TDP-43 levels at 28 days post blast. a ELISA, b Immunohistochemistry

Western blotting with anti-TDP43 (N-t) antibody showed no significant change at the molecular weight of 45 kDa, but revealed a significant increase of TDP43 in the blast group that was immunoblotted with anti-TDP43 (C-t) antibody (Fig.14a). Those changes were apparent at 60 kDa or 25 kDa, prompting questions as to whether blots might represent cleaved and/or dimeric forms of TDP43. To determine whether blast increases the cleaved TDP43, while the full length of TDP43 expression may not be altered significantly, we applied mass spectrometric analytical techniques. Briefly, the protein extractions underwent immunoprecipitation with 3 different anti-TDP43 antibodies. The eluate was run to a SDS-PAGE gel and was silver stained using a complete kit (ThermoFisher Scientific). The bands (Fig.14b) at 25, 45 and 60 kDa were cut and digested with trypsin and analyzed on Xevo G2-XS (WATERS) LC/MS systemR. The peptides were mapped to the expected amino acid sequence in the UNIFI (WATERS) software. Data exhibited the presence of TDP43 peptides with different coverages that indicated the fragments of TDP43 may play a role in cell development and regulation. TDP-43 proteinopathies include homeostatic imbalance between nuclear and cytoplasmic localization, aggregation of ubiquitinated and hyper-phosphorylated TDP-43, and an increase in protein truncation of cytoplasmic TDP-43.

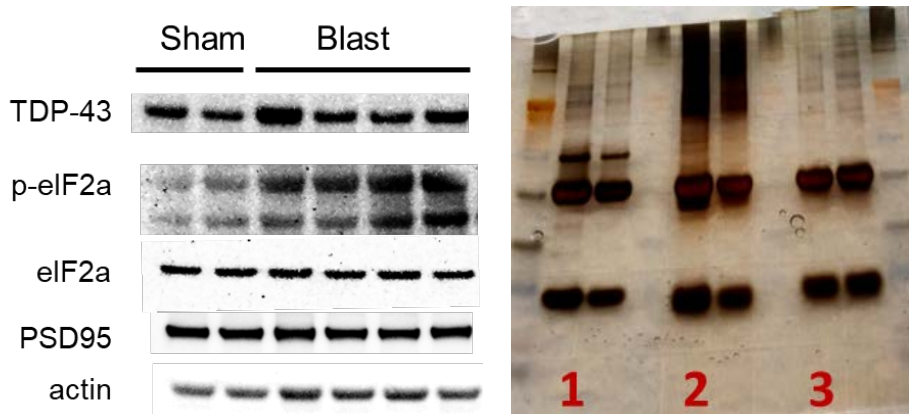


Fig. 14. TDP43 increased in the cortex at 28 days. (a) Western blotting, (b) silver stained gel contained anti-TDP-43 immunoprecipitated proteins

IV-2. Verify overexpression of TDP-43 altered neuronal development in cultured neurons

To address whether truncated TDP-43 is more toxic to the neuron full length TDP-43, we made several constructors such as pAAV-CAG-TDP43-GFP, pAAV-L7-TDP43-GFP, pAAV-myc-CAG-TDP43-GFP, pAAV-CAG-TDP43.208-GFP (truncated TDP-43 at c-terminal aa208.), pAAV-L7-TDP43.208-GFP and pAAV- Δ L7-TDP43-GFP (truncated L7).

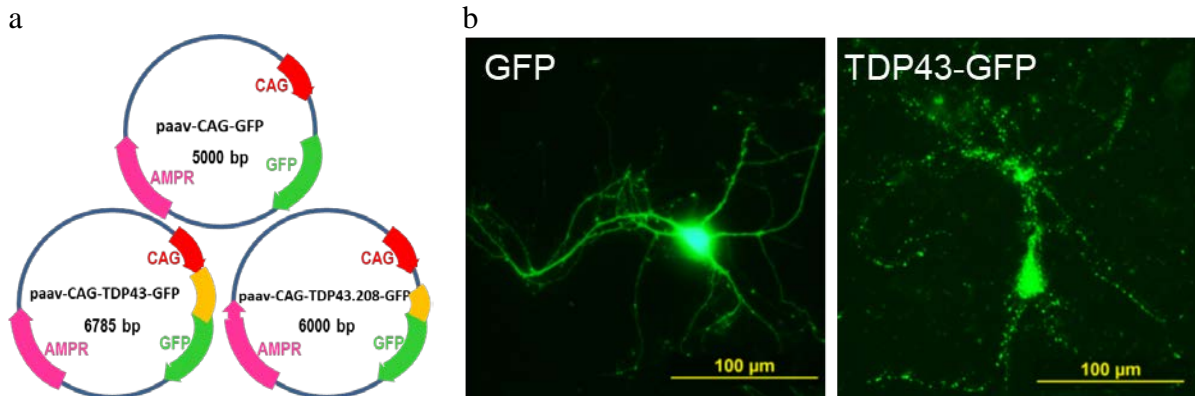


Fig. 15. The map of constructors (a) and primary neurons with TDP43 infection (b)

Initially, the Western blotting and qPCR analyses were used to determine whether TDP-43 or TDP43.208 can be overexpressed in the cultured mouse primary neurons at 2-5 days after transfection of pAAV constructor. To detect if overexpression of TDP-43 could impair neuronal development and synapse formation, we observed neuron morphology after applied viral guided genes, AAV-CAG-TDP43-GFP and AAV-CAG-TDP43.208-GFP (Fig. 15a) and AAV-L7-TDP43-GFP and AAV-L7-TDP43.208-GFP to primary cortical neurons and cerebellar Purkinje cells, respectively. Data showed that neurons with viral-GFP (control) infection appeared in a healthy condition, while neurons with viral-TDP43-GFP (overexpression of TDP-43) infection displayed very weak green fluorescence and appeared in a degenerative condition (Fig. 15b). The morphology of neurons with viral-TDP43.208 infection (data was not shown) is similar to that of control. Together, these results indicated that the full length TDP-43 is more toxic to neurons than that of truncated TDP43.208.

IV-3. Effects of regulating TDP-43 target genes on gene expression in neurons

To determine whether altered expression of TDP-43 can be a key pathophysiological mechanism leading to the secondary central auditory processing injuries, we employed a single-cell RNA sequencing assay combined with whole-cell patch-clamp recording to investigate the differentially expressed genes (DEG) triggered by upregulation of TDP-43. The following challenging technical methods (four steps) have been successfully accomplished.

- A. *Brain virus injection*: Briefly, anesthetized mice were placed in a stereotaxic frame. Craniotomies were made to allow AAV encoded gene to be injected bilaterally into the MGN. Mice received one of three agents of control (aav-cag-GFP), TDP43-FL (aav-cag-TDP43-GFP, full length of tdp-43) and TDP43-208 (aav-cag-TDP43.208-GFP,

truncated tdp-43) and were separated into three experimental groups. Mice were maintained to recover for 4 weeks after injection to allow maximal gene expression.

- B. *Single neuron collection*: Mice were euthanized at 28 days after injection and the brains were quickly removed after anesthetization with isoflurane. Slices containing MGN (400 μm) were cut as coronal sections using a vibrating blade microtome (Leica VT1000S, Leica Systems) and transferred to a holding chamber for recovery, and then transferred to a submersion recording chamber. GFP-positive neurons in the MGN were visualized under microscope (Olympus BX51), and each single cell was harvested by a whole-cell recording pipette. A total of 32 samples were evaluated; each sample contained five cells from 3 groups.
- C. *Cell processing for RNA extraction*: Five cells were pooled as a single sample that was processed for RNA extraction immediately after collection using the SMART-Seq HT Kit. Accorded to the manufacturer's instruction, these samples were processed to STOPPING POINT and stored at -20°C for next steps.
- D. *RNA-seq and analysis*: Library constructs and RNA sequencing were performed using an Illumina HiSeq 2000. Bioinformatics Analyses94 software was used to identify specific signaling pathways that are upregulated in each cell population following altered TDP-43 expression at the LIBD/JHU.

The overall RNA-seq results showed that, compared to the control neuron, 206 differentially expressed genes (DEGs) were identified in the TDP43-FL (Fig.15a) overexpressed neuron, and 261 DEGs were identified in the truncated TDP43 (TDP43-208) overexpressed neuron ($p < 0.01$, Fig.15b). Gene set enrichment analyses demonstrated that DEGs in TDP43-FL vs control were mostly significantly enriched in RNA binding processing (Fig.15c and e), including 'rRNA processing' ($p = 4.18\text{e-}04$, GO: 0006364), 'maturation of SSU-rRNA' ($p = 6.67\text{e-}04$, GO: 0030490), 'rRNA metabolic process' ($p = 1.08\text{e-}03$, GO: 0016072) and 'ribosome biogenesis' ($p = 1.18\text{e-}03$, GO: 0031347). The differential expression and GO analyses together suggested that Kri1 ($p = 6.36\text{e-}03$), Nol10 ($p = 4.44\text{e-}03$), Dcaf13 ($p = 1.02\text{e-}03$) and Tsr3 ($p = 4.76\text{e-}03$) were among the most biologically relevant genes for these RNA binding processing. In regard to TDP43-208 vs control (Fig.14 d and f), gene set enrichment analyses revealed that DEGs were mostly significantly enriched in 'regulation of action potential' ($p = 2.08\text{e-}04$, GO: 0001508), 'regulation of cell survival and apoptosis' ($p = 5.25\text{e-}04$, GO: 0034350), 'regulation of cell morphogenesis involved in differentiation' ($p = 1.33\text{e-}03$, GO: 0010769) and 'negative regulation of neuron projection development' ($p = 1.96\text{e-}03$, GO: 0010977).

Our findings indicate that blast exposure increases expression of TDP43 in brain tissue, which could also increase truncated TDP-43 fragments. Our electrophysiological data have shown that blast exposures impair the synaptic transmission in MGN-AU projections. Combined with the single-cell RNA-seq analyses, these results implicate that blast-induced central auditory processing disorders might be attributable to dysfunction of MGN-AU projections, which is caused by blast-induced overexpression of TDP43 and truncated TDP43 fragments leading to dysfunctional rRNA binding, impaired neuronal axonal development and neuronal firing, as well as neuronal survival and apoptosis.

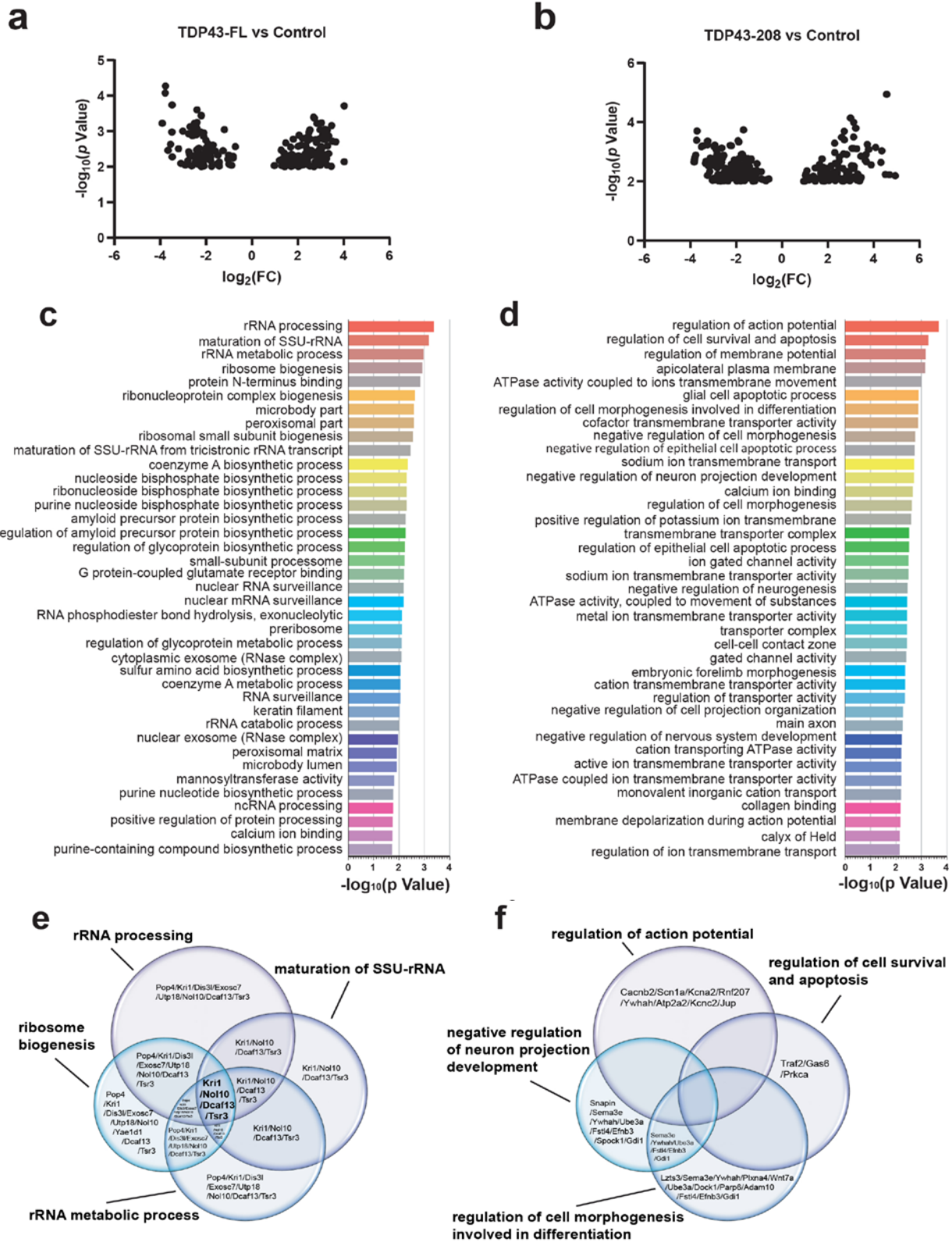


Fig. 15 Single neuron RNAseq analysis

V. Blast-induced protein changes in the cortex and cerebellum

To identify the effects of blast exposure on the proteomic profile in the mouse brain, a comparative proteomic analysis of the proteins at a global level was performed by using a mass spectrometry-based quantitative proteomics technology. A total of 36 mice were separated randomly into experimental treatment groups including tightly coupled double blast exposures (B) and sham controls (C). The investigation time intervals were 1, 7, 28 and 60 days after injury. The sham control groups were C1 (n=6), C28 (n=6) and C60 (n=3). The blast groups were B1 (n=6), B7 (n=6), B28 (n=6) and B60 (n=3). Brain tissues, cerebral cortex (ct) and cerebellum (cb) were processed for protein extraction and TMT-multiplex labeling. The peptide fractionation and nanospray LC/MS-MS analysis were performed by Poochon Scientific (Frederick, Maryland).

V-1. Characterize protein profiling change in the cortex after blast exposure

To identify the protein signature related to the blast injury, a total of 6069 proteins were quantitatively identified in this study and 3505 proteins were quantitatively identified in all 30 samples. Protein abundance in the cortical region of mice were compared among five experimental groups (C1, B1, B7, C28 and B28, 6 mice for each group). The proteomic profiles are illustrated in the heat maps (Fig.16 a and b). Fig.16b shows the relative abundance of 84 proteins identified across 5 groups of 30 cortical samples which are changed by at least 25% in one treatment in comparison with C1 (fold change >25%, p-Value <0.05, n=6). The distribution of the differentially expressed protein (DEPs) is presented as a Venn diagram (Fig.17), 1399 DEPs (39.91% of the total proteins) were identified with 627 (44.82%) up-regulated and 772 (55.18%) down-regulated proteins in B1 vs C1. In contrast, 1546 DEPs (44.11% of total proteins) were identified with 804 (52.01%) up-regulated and 742 (47.99%) down-regulated proteins in B7 vs C1. Finally, 555 DEPs (15.83% of total proteins) were identified with 252 (45.41%) up-regulated and 303 (54.59%) down-regulated proteins in B28 vs C28. There are 125 proteins are shared among D1, D7 and D28.

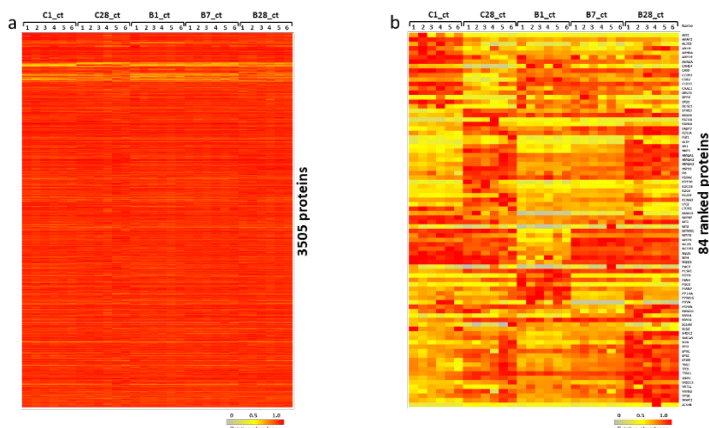


Fig.16. Heat map depicting the proteomes of mouse's cortex. (a) the relative abundance of 3505 proteins, (b) the relative abundance of ranked 84 proteins identified across 5 groups of 30 samples. The color key indicates the relative abundance of each protein (0 to 1.0)

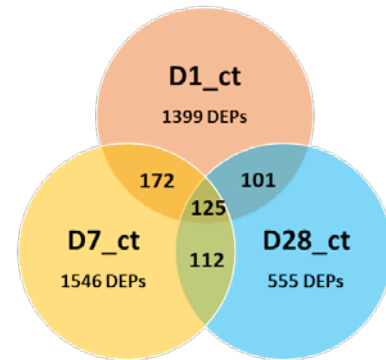


Fig.17. Venn diagram depicting DEPs in the cortex at 1, 7 and 27 days post-blast.

Volcano plots showed that 26 proteins were changed by at least 1.25-fold in the blast-exposed mice (B1 group comparing to the C1, $p < 0.05$, Fig.18a), while 19 proteins changed significantly in B7 vs C1 (Fig.8b), and 38 proteins changed in B28 vs C28 (Fig.18c).

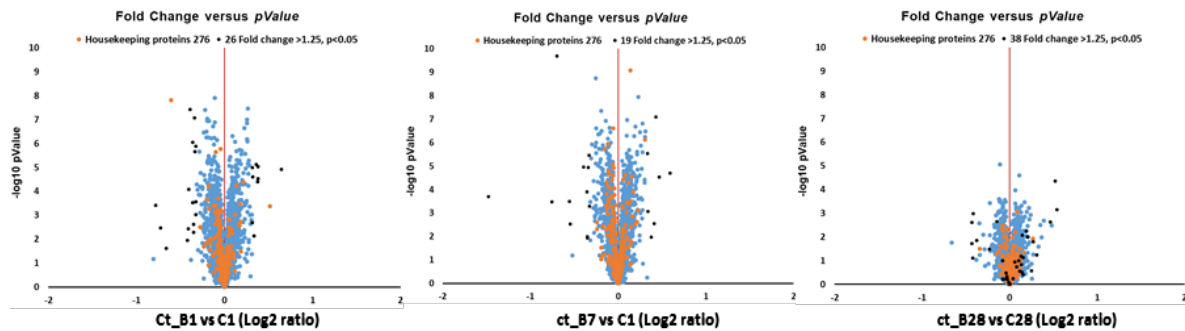


Fig.18. Volcano plots for the $\log_2(\text{fold change})$ and $-\log_{10}(\text{p value})$ of all proteins in B vs C at 1, 7 and 28 days after blast exposure.

V-2. Characterize protein profiling change in the cerebellum after blast exposure

We have quantitatively identified a total of 4993 proteins in the cerebellum of mouse among six experimental groups. There were C1 (n=5), B1 (n=5), C28 (n=5), B28 (n=6), C60 (n=3) and B60 (n=3). The proteomic profiles are illustrated in the heat maps (Fig.19 a and b). Fig 19b shows the relative abundance of 414 proteins identified across 6 groups of 27 samples which are ranked (fold change >10%, $p < 0.05$, n=3) in C60 group comparing to C28 group. Very interestingly, the proteomic pattern of B28 was remarkably different from that of C28, but was similar to that of C60 and B60. This finding potentially indicates that blast injury can accelerate aging related protein expressions.

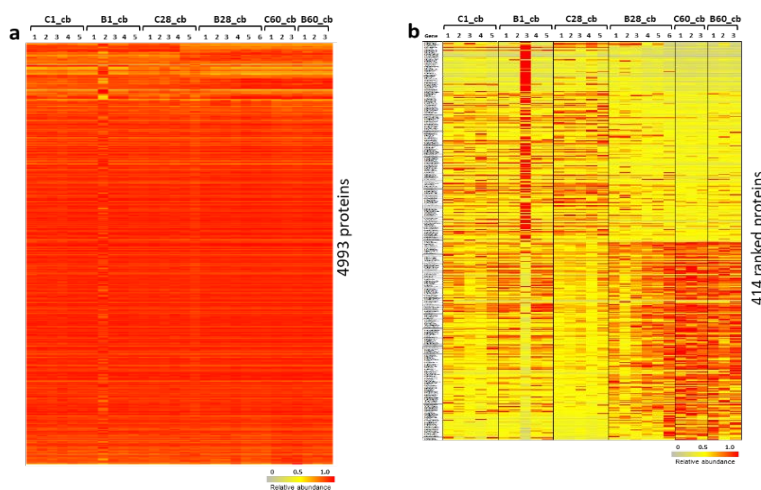


Fig.19. Heat map depicting the proteomes of mouse's cerebellum. (a) the relative abundance of 4993 proteins, (b) the relative abundance of ranked 414 proteins identified across 6 groups of 27 samples. The color key indicates the relative abundance of each protein (0 to 1.0).

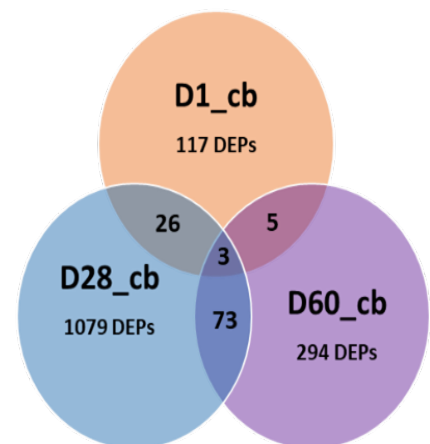


Fig.21. Venn diagram depicting DEPs in the cerebellum at 1, 28 and 60 days post-blast.

To identify the variation of proteins in mouse's cerebellum, the relative abundance of 4993 proteins were analyzed. Volcano plots (Fig.20) showed that 9 proteins were changed by at least 10%, $p < 0.05$ in the B1 group comparing to the C1 group (Fig.20a), while 204 proteins changed in B28 vs C28 (Fig.20b), and 23 proteins changed in B60 vs C60 (Fig.20c). The distribution of the differentially expressed proteins (DEPs) is presented by a Venn diagram (Fig.21), 117 DEPs (2.34% of the total proteins) were identified with 69 (58.97%) up-regulation and 48 (41.03%) down-regulated proteins in B1 vs C1. In contrast, 1079 DEPs (21.61% of total proteins) were identified with 469 (43.47%) up-regulation and 610 (56.53%) down-regulated proteins in B28 vs C28. And 249 DEPs (4.99% of total proteins) were identified with 119 (40.48%) up-regulation and 175 (59.52%) down-regulated proteins in B60 vs C60. There are 29 proteins are shared between D1 and D28.

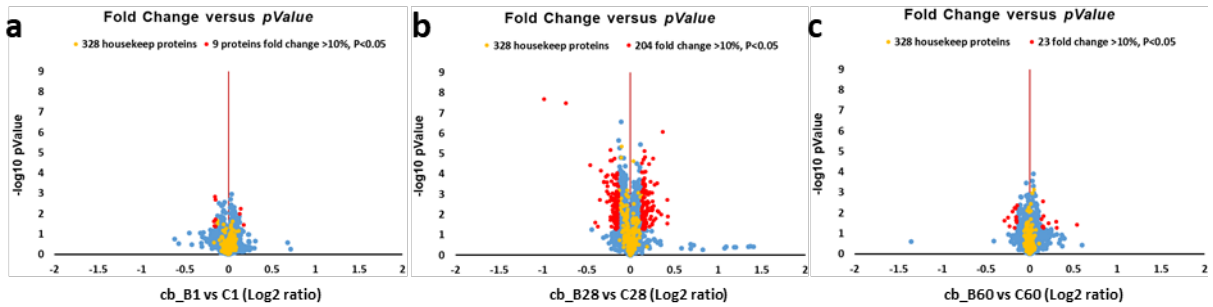


Fig.20. Volcano plots for the $\log_2(\text{fold change})$ and $-\log_{10}(\text{p value})$ of all proteins in B vs C at 1, 28 and 60 days after blast exposure.

We also identified the DEPs among C1, C28 and C60 groups, which included three ages (10, 14 and 18 wks) of normal control mice. Volcano plots showed that 83 proteins were changed by at least 10%, $p < 0.05$ in the C2 group comparing to the C1 group (Fig.22a), while 369 proteins changed in C60 vs C1 (Fig.22b). Four particular proteins, Hmgb2, Cdh13, Ly6h and Camkv, have been identified among those three age groups (Fig.23).

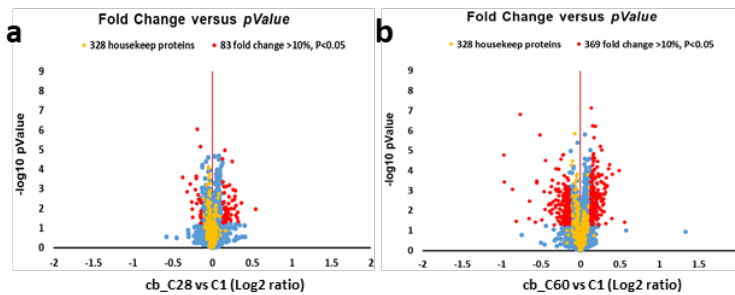


Fig.22. Volcano plots for the $\log_2(\text{fold change})$ and $-\log_{10}(\text{p value})$ of all proteins in C28 vs C1 and C60 vs C1.

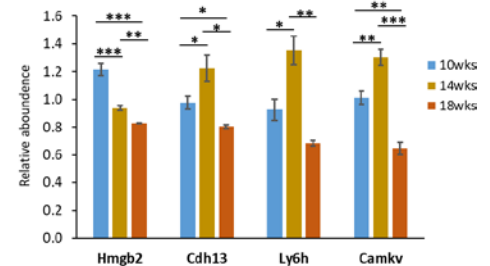


Fig. 23. Age related DEPs in the cerebellum of sham mouse, * $p < 0.05$, ** $p < 0.005$, *** $p < 0.001$

V-3. Validation of blast-induced DEPs in the cortex by Western blot or ELISA

We also used Western blotting or/and ELISA analysis to validate some of DEPs changes seen with proteomic analysis. The following proteins are presynaptic or postsynaptic proteins associated with synaptic plasticity, as well as neuron-derived neurotrophic factor in the cortex region (Fig.24).

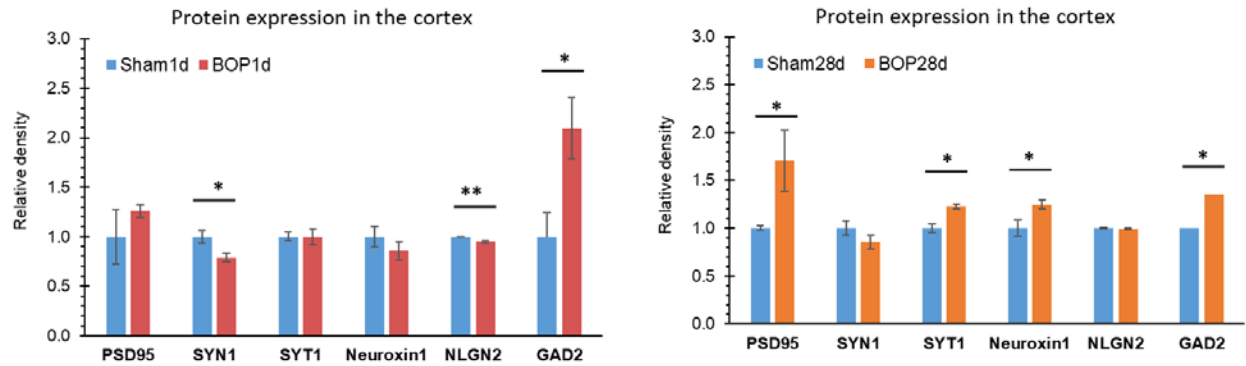


Fig. 24. Blast-induced protein changes in the cortex at 1 or 28 days bTBI

- The postsynaptic density (PSD) serves as a signaling apparatus. It has been proposed to concentrate and organize neurotransmitter receptors in the synaptic cleft. Compared to the sham controls, PSD95 (DLG4), PSD93 (DLG2) and DLG3 increased significantly at 28 days post-blast. They also increased slightly at an acute phase, but no statistical differences were observed. PSD97 was unchanged throughout. As seen with PSD-95/SAP90-binding proteins, DLGP3 and DLGP4 also increased ($p < 0.01$) at 1 day post-blast, but no changes for DLGP1 and DLGP2 were detected.
- Neuroligin (NLGN) is a cell adhesion protein on the postsynaptic membrane that mediates the formation and maintenance of synapses between neurons. NLGN1 localizes at excitatory synapses, NLGN2 at inhibitory synapses, and NLGN3 at both.
- NLGN2 and NLGN3 decreased ($p < 0.005$) at an acute phase, but no changes in NLGN1 were seen. Reduction in the levels of neuroligins 1, 2 and 3 results in a strong reduction of inhibitory input, but little reduction in excitatory input.
- The N-methyl-D-aspartate receptors (NMDA) are also associated with synaptic plasticity. NMDARs (also named GluN or GRIN) are composed of two subunits. Ca^{2+} flux through GluN is thought to be critical in synaptic activities. Compared to the sham controls, GluN2B increased ($p < 0.005$) at 1 days but decreased at 28 days post-blast. There were no changes in GluN1 and GluN2A.
- The α -amino-3-hydroxy-5-methyl-4-isoxazolepropionic acid receptor (AMPA) is a non-NMDA-type receptor for glutamate. AMPARs are composed of four types of subunits encoded by genes GRIA (also named GluA or GluR). AMPARs are integral to synaptic plasticity at many postsynaptic membranes that mediate fast synaptic transmission in the CNS. Compared to the sham controls, GluA2 and GluA3 decreased ($p < 0.05$) at 28 days post-blast, but no changes were observed in GluA1 and GluA4.
- Synaptotagmins (SYT) serve as sensors for calcium ions in the process of vesicular trafficking and exocytosis. SYT1, localized in the membrane of the pre-synaptic axon terminal, binds to Ca^{2+} and participates in triggering neurotransmitter release. Compared to the sham controls, SYT1 decreased significantly at 1 and 7 days post-blast, while SYT2 increase increased ($p < 0.05$) at 28 days post-blast.

- Synapsins (SYN) bind synaptic vesicles to components of the cytoskeleton which prevents them from migrating to the presynaptic membrane and releasing neurotransmitter. Compared to the sham controls, SYN1 decreased significantly ($p < 0.001$) at both acute phase and chronic phase, while SYN2 decreased ($p < 0.05$) at 28 days post-blast. SYN1 decreased significantly ($p < 0.001$) at both acute phase and chronic phase, while SYN2 decreased ($p < 0.05$) at 28 days post-blast.
- Synaptophysin (SYP) is a synaptic vesicle glycoprotein, and was unchanged following blast exposure.
- Neurotrophic factors (NTFs) comprise a family of biomolecules that support the growth, survival, and differentiation of both developing and mature neurons. Compared to the sham controls, neurotrophic tyrosine kinase receptor type 2 (NTRK2) decreased at 7 days post-blast, but increased at 28 days post-blast. BDNF decreased in both acute and chronic phases.
- Glutamate decarboxylase 65 (GAD2), expression in the GABAergic neurons is localized to nerve terminals and synapses. GAD2 is predominantly found in an inactive state. Our data showed that GAD2 increased significantly at acute and chronic injury phases after blast exposure. The results reveals that blast injury can activate GABA neurotransmission.

What opportunities for training and professional development has the project provided?

Technical skill development includes:

- ABR and DPOAE testing
- Precise brain region injection
- Design an AAV-gene-GFP
- Primary neuronal culturing
- Brain section cutting, imaging and data analysis
- Patching single neuron
- Whole-cell patch-clamp electrophysiological recording
- RNA extraction
- Single cell RNAseq analysis

How were the results disseminated to communities of interest?

The PIs, Research associates, Postdoctoral fellows, and technicians attended scientific meetings and presented our finding at the Society for Neuroscience Symposium, Military Health System Research Symposium, National Capital Area TBI symposium as well as the Japan US technical information exchange forum.

4. IMPACT:

What was the impact on the development of the principal discipline(s) of the project?

Nothing to report.

What was the impact on other disciplines?

Nothing to report.

What was the impact on technology transfer?

Nothing to report.

What was the impact on society beyond science and technology?

This project contributed to our comprehensive understanding of how blast exposure affects brain regions that are closely associated with sound signaling processing. Impairment by shockwaves of synaptic plasticity does not only impact auditory function, but also potentially similarly disrupts learning and memory. Evidence of the structural and molecular components of injury is essential for the targeted development of the most suitable therapies for auditory/vestibular deficits suffered by individuals, such as service men and women, who risk exposure to blast or other concussive insults in the field.

5. CHANGES/PROBLEMS:

Nothing to report.

6. PRODUCTS:

- **Publications, conference papers, and presentations**
Journal publications.

A manuscript, entitled “ Impact of blast exposure on synaptic plasticity in mouse” is ready to submit.

Books or other non-periodical, one-time publications.

Nothing to report.

- **Website(s) or other Internet site(s)**

Nothing to report

- **Technologies or techniques**

Nothing to report

- **Inventions, patent applications, and/or licenses**

Nothing to report

7. PARTICIPANTS & OTHER COLLABORATING ORGANIZATIONS

What individuals have worked on the project?

Dr. Joseph B. Long, PI
Dr. Ying Wang, Co-PI
Dr. Yanling Wei, Research Associate
Ms. Donna Wilder, Research Manager

What other organizations were involved as partners?

Lieber Institute for Brain Development at Johns Hopkins University
855 N Wolfe St Suite 300, Baltimore, MD 21205

8. SPECIAL REPORTING REQUIREMENTS

The QuadChart is attached

9. APPENDICES: